Available online at
www.ijacskros.com

Indian Journal of Advances in Chemical Science

Indian Journal of Advances in Chemical Science S1 (2016) 152-156

# Wavelet Transform based Evaluation of Surface Images in High Speed Turning of Ti-6al-4v

**J. S. Vishwanatha*, P. Srinivasa Pai, Grynal D'Mello**

*Department of Mechanical Engineering, NMAM Institute of Technology, Udupi, Karnataka, India.*

*Received 07th April 2016; Revised 14th May 2016; Accepted 15th May 2016*

***ABSTRACT***

*This paper presents the threshold based image denoising methods for turned images using hard threshold, soft threshold, and an improved threshold method. The turning experiments were carried out on a CNC turning center, on Ti-6Al-4V bars under different cutting conditions namely speed, feed, and depth of cut. A computer vision system has been used to capture different turned surface images. The denoising results of the new improved threshold method is superior than the soft- and hard-threshold methods with minimum mean square error and maximum peak signal to noise ratio. Wavelet packet transform have been used for extracting the statistical features namely mean, variance, standard deviation, skewness, and kurtosis from the denoised turned surface images. These statistical features along with cutting conditions namely speed, feed rate, and depth of cut along with tool flank wear have been used as inputs to radial basis function neural network for modeling and prediction of surface roughness parameter ($R_a$) from the turned images.*

***Key words:*** *Wavelet transform, Image denoising, Mean square error, Peak signal to noise ratio, Radial basis function neural network.*

## 1. INTRODUCTION

Surface roughness is the measure of finely spaced micro irregularities produced during machining process. Surface quality is one of the most important requirements for the manufacturing industry [1]. Turning is a widely used machining operation in the manufacturing process. The surface roughness of turned parts is usually measured by contact and non-contact methods [2]. Several investigations have been performed to inspect surface roughness of a work piece based on computer vision technology [1-3]. Titanium alloys are extensively used in aerospace, biomedical applications because of its outstanding mechanical properties and they are used in corrosive environments [3].

Digital images are often degraded by noise during the acquisition or transmission. The removing of noise from any affected image is referred to as denoising. The goal of denoising is to remove the noise and to retain the important image features as much as possible [4]. The denoising of images using the traditional soft and hard threshold has some disadvantages. The discontinuous nature of hard threshold function causes oscillation in signal reconstruction, the denoised image has the Pseudo-Gibbs phenomenon and other visual distortion. The differential coefficients of soft threshold function are not continuous and there exists a constant deviation between the estimates of wavelet coefficients and the real wavelet coefficients as well as denoised image causes edge blur [4]. To overcome these disadvantages, various improvement methods have been proposed, such as semi-soft threshold method and multi threshold method. [7].

This study focuses on threshold based image denoising for turned images using hard threshold, soft threshold, and an improved threshold method. All the three methods of image denoising techniques are compared in terms of minimum mean square error (MSE) and maximum peak signal to noise ratio (PSNR). Wavelet packet transform (WPT) have been used for extracting the statistical features namely mean, variance, standard deviation, skewness, and kurtosis from the turned denoised surface images. These statistical features along with cutting conditions namely speed, feed rate, and depth of cut with tool flank wear have been used as inputs to radial basis function neural network (RBFNN) for modeling and prediction of surface roughness parameter ($R_a$) from the turned images.

This paper is organized as follows. Section 1 presents the introduction, Section 2 presents experimental

*Corresponding Author:
*E-mail: vishwajs@nitte.edu.in*

set up, Section 3 describes wavelet based denoising schemes, Section 4 presents WPT based feature extraction, Section 5 explains RBFNN for modeling and prediction of surface roughness of turned surfaces.

Section 6 explains results and discussion; conclusions are given in Section 7.

## 2. EXPERIMENTAL SET UP

The turning experiments have been carried out using HMT make- Stallion100SU CNC turning center at different speeds, feeds, and depth of cuts. Ti-6Al-4V bar of 50 mm diameter and 200 mm length is chosen as the work material for turning experiments. Uncoated carbide inserts 883 with MR4 chip breaker (SECO make) and PCLNL 2020 K12 (SECO make) tool holder is used. Experiments were conducted under dry cutting conditions for speeds of 150, 175, 200 m/min, feed of 0.15, 0.2, 0.25 mm/rev and depth of cut of 0.8, 1, and 1.2 mm. A total 27 set of experiments have been carried out. Length of the cut is 48 mm and after each cut, the tool flank wear is measured. Turning is carried out till the flank wear reached 0.4 mm. Measurement of flank wear is done using Mitutoyo Tool Maker's Microscope (TM 505/510) which has a magnification of X15, with provision for measurement using micrometers in X and Y direction with a least count of 0.005 mm.

The turned surface images have been captured using a computer vision system, which consists of a digital camera, lighting arrangement, work table, and PC for image processing as shown in Figure 1. The component is mounted on the worktable and the light source is arranged in such a way that the illumination should be uniform. A distance of approximately 25 cm is maintained between the work piece and the camera throughout the experimentation. The captured image using digital camera is saved with an image resolution of 256 × 256 pixels.

## 3. WAVELET BASED DENOISING SCHEMES

Image denoising is referred as extracting the noise from any affected image. The denoising purpose is to extract the noise and to retain the required image features as much as desirable [5]. Consider an original image signal f (x, y) of size 256 × 256 pixels resolution. Add white Gaussian noise n (x, y) to original image in order to get noisy image g (X, Y) [6].

$$g(X, Y) = f(X, Y) + n(X, Y) \tag{1}$$

The wavelet transform is a linear transformation and the coefficients of the image signal are composed into two parts.

$$W_g(X, Y) = W_f(X, Y) + W_n(X, Y) \tag{2}$$

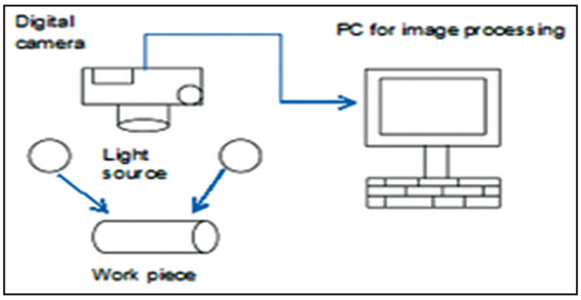


**Figure 1:** Schematic layout of computer vision system.

Where $W_g$, $W_f$, and $W_n$ represents wavelet transform coefficients of g, f, and n, respectively. The desire of wavelet based image denoising is to get estimative wavelet coefficients $\hat{W}_f$ from the expected image wavelet coefficient $W_f$ of the noisy image.

### *3.1. Selection of Threshold Method*

There are various wavelet thresholding methods. Hard- and soft-thresholding are the important methods of wavelet thresholding. In hard threshold method, a range of coefficients of wavelet transform are set to zero and retain the remaining wavelet coefficients.

The method of hard threshold is given by:

$$\hat{W}_f(x, y) = \begin{cases} w_g(x, y) & |w_g(x, y)| \geq T \\ 0 & |w_g(x, y)| < T \end{cases} \tag{3}$$

In soft threshold method, a range of coefficients of wavelet transform are set to zero and the remaining wavelet coefficients are compress. The method of soft threshold is given by:

$$\hat{W}_f(X, Y) = \begin{cases} \mathrm{sgn}(w_g(x, y)) & \\ (|w_g(x, y)| - T) & |w_g(x, y)| \geq T \\ 0 & |w_g(x, y)| < T \end{cases} \tag{4}$$

Where T is the threshold.

These two methods are generally used in practice and give reasonable results, but these methods have some defects. The irregular nature of hard threshold method causes fluctuation in signal reconstruction, the denoised image has the Pseudo-Gibbs phenomenon, and other visible distortion. The wavelet transform coefficients of soft threshold method are not regular and there exists a constant variation between the estimates of wavelet coefficients and the real wavelet coefficients and also the denoised image appear edge blur. To overcome these defects of hard- and soft-threshold methods, an improved threshold method of denoising is proposed in [4].

$$\hat{W}_f(x,y) = \begin{cases} \operatorname{sgn}\left(w_g(x,y)\right) \left( \left|w_g(x,y)\right| - \dfrac{T}{(\exp(\left|\dfrac{w_g(x,y)-T}{q}\right|)^p)} \right) & \left|w_g(x,y)\right| \geq T \\ 0 & \left|w_g(x,y)\right| < T \end{cases} \quad (5)$$

p and q are integers, the improved threshold method has following quality, when q tends to 0, the threshold method is near to the hard threshold method, when q tends to be infinite, the threshold method is near to the soft threshold method. This method overcomes the irregular nature of the hard threshold, and also the value of PSNR can be increased. It also largely reduces the variation, so that the constant variation between $W_g(X, Y)$ and $W_f(X, Y)$ in the soft threshold method is overcome [4].

### *3.2. Threshold Estimation*

In addition to the selection of threshold method, the another important aspect in wavelet threshold image denoising is the estimation of the threshold. The classic threshold estimation methods include that suggested by Donoho and Johnstone, but they are not optimal [4]. The threshold is given by:

$$T = \sigma\sqrt{2\ln(N)} \quad (6)$$

Threshold interval based on zero mean normal distribution is set to T=3σ~4σ, where σ is the standard deviation of the noise and N is the sample number of observations.

The new threshold is determined by:

$$T_{new} = k_j\sigma\sqrt{2\ln(N)} / \log(h+1) \quad (7)$$

Where h is the level of decomposition of wavelet transform. To minimize distortion take $k_j$ as 1 in high high (HH) frequency band and $k_j$ as √2 in high low (HL), low high (LH) frequency band.

## 4. WPT BASED FEATURE EXTRACTION

WPT is an expansion of the wavelet transformation. Only low-frequency components of the signal are decomposed in wavelet transformation. Compared to that, both the low- and high-frequency components of decomposition take place in WPT. A WPT effectively extracts the specific frequency components and hence improves the frequency resolution [8]. In wavelet packet decomposition technique, an image is decomposed into four decomposition coefficients in the first level. Further, these four coefficients are again divided into 16 decomposition coefficients in the second level. Since two levels of decomposition are used, there are a total of 20 (4+16) decomposition coefficients. In this technique, all detailed coefficients are used for next level of decomposition. Energy details represent the energy of the various decomposition coefficients. Based on the highest energy level of the decomposition coefficient, the textural features are extracted. "$a_4$" which is a second level coefficient possesses maximum energy, when compared to other coefficients hence, it is used to extract textural features from an image.

The textural features namely mean, variance, skewness, kurtosis, and standard deviation were extracted from the $a_4$, wavelet packet coefficients obtained from the acquired images, sample values of which are given in Table 1. These textural features provide information about the surface in the images.

## 5. RBFNN FOR MODELLING AND PREDICTION OF SURFACE ROUGHNESS OF TURNED SURFACES

RBFNN has an input layer, an output layer, and a hidden layer composed of RBF neurons. The input layer consists of source nodes that connect the network to its environment. The second layer of network is the hidden layer, applies a nonlinear transformation from the input space to the hidden space. Each node of the hidden layer has two parameters, a center $x_j$ and a width $\sigma_j$. The neuron in the hidden layer consist of Gaussian transfer function

$$\varnothing j(x) = e^{\frac{-\|xj-\zeta i\|}{2\sigma j^2}}$$

Where j=1, 2.....c, c is the number of centers. These centers are used to analyze with the network input vector to outcome a radially symmetrical response. The precision properties of the interpolating function are controlled by the width. Feedback of the hidden layer are scaled by the contact weights of the output layer and then connected to produce the network output [9]. To predict the surface roughness from the turned surfaces, five textural features along with cutting conditions and tool flank wear are used as inputs to RBF model to get surface roughness

**Table 1:** Textural features for cutting condition: 150 m/min speed, 0.15 mm/rev feed and 0.8 mm depth of cut.

| Mean | Variance | Skewness | Kurtosis | Standard deviation |
|---|---|---|---|---|
| 99.7887 | 302.4162 | 0.1368 | 2.6871 | 17.0949 |
| 83.462 | 388.9806 | 0.4196 | 2.9684 | 19.4666 |
| 113.8285 | 372.1252 | 0.6012 | 3.2087 | 18.7881 |
| 90.2636 | 406.7263 | 0.363 | 2.734 | 19.9372 |
| 113.3814 | 260.7317 | 0.2609 | 2.9128 | 15.7431 |

parameter ($R_a$) as output. The feature values are normalized and randomized to achieve better prediction of surface roughness. There are a total of 27 set of experiments, containing 289 images out of which 85% of the images have been used for training the model and remaining 15% for testing the trained model. Figure 2 shows the RBFNN model used in this work.

## 6. RESULTS AND DISCUSSION

To check the performance of the improved threshold method, a standard turned image of 256 × 256 pixel resolution is considered. Noisy images with distinct noise levels have been develop by adding white Gaussian noise, to the original noisy turned images. The results of proposed method that use of the new threshold for image denoising have been correlated with that of hard- and soft-threshold methods. A "bior2.4" wavelet used with two level wavelet decomposition. The denoising results of improved threshold method is superior than the soft and hard threshold methods with minimum MSE and maximum PSNR as shown in Table 2. PSNR is given by:

$$PSNR = 10\lg\left(\frac{(M \times N) \times \max(\hat{f}_{i,j})^2}{\sum_{i,j}(f_{i,j} - \hat{f}_{i,j})^2}\right) \quad (8)$$

MSE is defined as:

$$MSE = \frac{1}{MN}\sum_{i=0}^{M-1}\sum_{j=0}^{N-1}((f_{i,j} - \hat{f}_{i,j})^2) \quad (9)$$

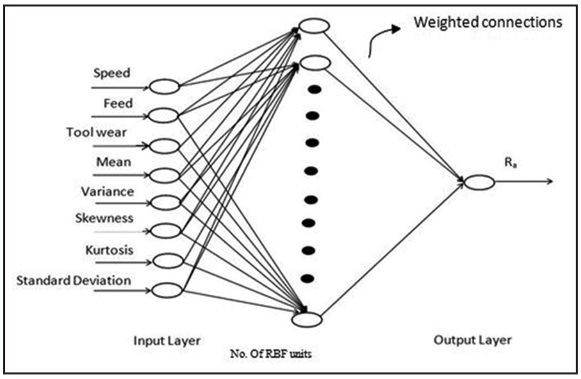


**Figure 2:** Radial basis function neural network model.

Where, f is original image and $\hat{f}$ is denoised image.

MxN is the pixel resolution of the image.

For prediction of surface roughness using RBFNN simulation parameters; η=0.85 and α = 0.05; have been maintained constant during the training of RBF network. The number of epochs was set to 1000. The network goal is fixed as 0.001. The width of the RBF units have been chosen by trial and error method based on the maximum prediction accuracy.

The training has been done using different widths of 0.1, 0.12, 0.14, 0.16, and 0.18. Table 3 shows the testing results for test samples for different number of RBF neurons selected randomly, out of which maximum prediction accuracy has been obtained for width of 0.18 and no. of RBF neurons of 55. The maximum prediction accuracy for test data is 95.14%.

## 7. CONCLUSION

This paper proposed a threshold based image denoising for turned images using hard threshold, soft threshold, and an improved threshold method and an improved threshold method. In addition, a best threshold that fits to all decomposition levels is described. WPT have been used for decomposing the images. Textural features namely mean, variance, standard deviation, skewness, and kurtosis have been extracted from wavelet packet coefficients from the denoised turned surface images. RBF neural networks have been applied for modeling and prediction of $R_a$ using these features. The following conclusions can be drawn:

a. The new improved threshold method is preferable than the soft and hard threshold method with minimal MSE and maximum PSNR.
b. The textural features extracted from the WPT coefficients results in better prediction accuracy from RBFNN model.
c. RBFNN are effective in surface roughness prediction for a width of 0.18 and 55 centers with a maximum prediction accuracy of 95.14% for test data.

**Table 2:** De-noising results using different threshold methods.

| Standard deviation of noise (σ) | Hard threshold | | Soft threshold | | Improved threshold | |
|---|---|---|---|---|---|---|
| | PSNR | MSE | PSNR | MSE | PSNR | MSE |
| 10 | 23.0072 | 31.090 | 16.0401 | 39.372 | 24.1384 | 13.533 |
| 15 | 20.4368 | 31.910 | 13.8794 | 40.463 | 23.7185 | 15.718 |
| 20 | 17.1040 | 40.252 | 12.3491 | 40.599 | 20.3720 | 23.756 |
| 25 | 14.6103 | 45.611 | 11.5054 | 54.673 | 16.0231 | 26.723 |

MSE=Mean square error, PSNR=Peak signal to noise ratio

**Table 3:** Performance of RBF model (no. of RBF neurons selected randomly).

| Number of RBF neurons (%) | 45 | 50 | 55 | 60 | 65 |
|---|---|---|---|---|---|
| Training accuracy | 95.546 | 94.331 | 95.238 | 93.117 | 90.688 |
| Testing accuracy | 90.476 | 90.476 | 95.141 | 92.857 | 90.476 |

RBF=Radial basis function


## 8. ACKNOWLEDGMENT

The Project has been funded by The Institution of Engineers (India), 8 Gokhale Road, Kolkata, 700 020 under R&D Grant-in-Aid scheme.


## 9. REFERENCES


1. P. Morala-Argüello, J. Barreiro, E. Alegre, (2012) A evaluation of surface roughness classes by computer vision using wavelet transform in the frequency domain, ***International Journal of Advanced Manufacturing Technology,*** **59**: 213-220.
2. B. Y. Lee, Y. S. Tarng, (2001) Surface roughness inspection by computer vision in turning operations, ***International Journal of Machine Tools and Manufacture,*** **41**: 1251-1263.
3. S. Ramesh, L. Karunamoorthy, K. Palanikumar, (2012) Measurement and analysis of surface roughness in turning of aerospace titanium alloy (gr5), ***Measurement,*** **45**: 1266-1276.
4. C. Guanguan, Y. Guihong, (2014) The application of the improved threshold method in wavelet image denoising, ***Advanced Materials Research,*** **1039**: 280-285.
5. A. Jaiswal, J. Upadhyay, A. Somkuwar, (2014) Image denoising and quality measurements by using filtering and wavelet based techniques, ***International Journal of Electronics and Communication,*** **68**: 699-705.
6. T. Hui, L. Zengli, C. Lin, C. Zaiyu, (2013) Wavelet image denoising based on the new threshold function, ***Proceedings of the 2nd International Conference on Computer Science and Electronics Engineering,*** p2749-2752.
7. S. Sudha, G. R. Suresh, R. Sukanesh, (2007) Wavelet based image denoising using adaptive thresholding, ***Conference on Computational Intelligence and Multimedia Applications,*** **3**: 296-300.
8. J. Xi, M. Zhang, L. Jiang, (2012) Analysis of tool wear condition based on logarithm energy entropy and wavelet packet transformation, ***3rd International Conference on Intelligent Control and Information Processing,*** **15-17**: 22-25.
9. S. Haykin. (2009), ***Neural Networks a Comprehensive Foundation,*** New Delhi: Pearson Education.


***Bibliographical Sketch**

*Vishwanatha J S is currently working as an assistant professor in the Department of Mechanical engineering, NMAM Institute of Technology, Nitte. He has total 5 years of teaching experience and 2 years of industrial experience as a Jr.CAD engineer in Pixel Infotek Pvt. Limited, Bengaluru. His area of interests includes Design of Machine Elements, Kinematics of Machines, and Finite Element Methods. Currently, he is pursuing Ph.D in the field of metal machining and image processing.*